

Mössbauer study of crystallographic and magnetic phase transitions, phonon softening, and hyperfine interactions in $\text{Zr}(\text{Al}_x\text{Fe}_{1-x})_2$

I. Nowik

Racah Institute of Physics, Hebrew University, Jerusalem 91904, Israel

I. Jacob

Department of Nuclear Engineering, Ben Gurion University of the Negev, 84105 Beer-Sheva, Israel

R. Moreh

*Department of Physics, Ben Gurion University of the Negev, 84105 Beer-Sheva, Israel
and Nuclear Research Center-Negev, 84105 Beer-Sheva, Israel*

(Received 9 June 1992; revised manuscript received 31 August 1992)

Mössbauer-spectroscopy studies of ^{57}Fe in $\text{Zr}(\text{Al}_x\text{Fe}_{1-x})_2$ ($x=0-0.825$) at various temperatures, from 90 to 612 K have been performed. For $x < 0.25$ the systems are of cubic Laves phase structure and order magnetically above room temperature. Above $x = 0.25$ the systems have a hexagonal structure and do not order magnetically above 90 K. The Mössbauer spectra in the paramagnetic state are all very well described by a model that assumes that the isomer shift and quadrupole interaction are linearly dependent on the number of Al first-nearest neighbors to the iron nucleus (0.056 mm/s and -7% per Al neighbor, respectively). The samples $x=0.083$, 0.167, and 0.20 according to the measured Mössbauer recoil-free fractions, display increasing phonon softening. The effective Debye temperature decreased from $\Theta_D \approx 440(30)$ K for $x=0$ to $\Theta_D \approx 310(30)$ K for $x=0.2$. The compounds with $x \geq 0.25$ harden again and Θ_D increases to 395(20) K.

I. INTRODUCTION

The rare-earth or Zr Laves phase compounds exhibit a wide variety of magnetic phenomena.¹ Mixed systems of the $\text{Zr}(\text{Al}_x\text{Fe}_{1-x})_2$ type exhibit ferromagnetism, spin-glass structure and crystallographic cubic (C15)-hexagonal (C14) phase transitions.² Recently it was suggested³ that $\text{Zr}(\text{Al}_x\text{Fe}_{1-x})_2$ may also exhibit phonon softening for low values of Al concentrations. Since Mössbauer spectroscopy of ^{57}Fe yields information on crystallographic structure (through quadrupole interactions), on magnetic order (through the magnetic hyperfine interactions), and on local vibrational amplitudes (through the recoil-free fraction), it was tempting to study in great detail $\text{Zr}(\text{Al}_x\text{Fe}_{1-x})_2$ in a wide range of temperatures and compositions.

II. EXPERIMENTAL DETAILS

The $\text{Zr}(\text{Al}_x\text{Fe}_{1-x})_2$ ($x=0, 0.04, 0.083, 0.167, 0.2, 0.3, 0.4, 0.5, 0.6, 0.7, 0.825$) intermetallic compounds were prepared in an arc furnace under an argon atmosphere by melting the weighted fraction of the pure metals on a water-cooled copper hearth. The Laves-phase structure of all the intermetallics was confirmed by x-ray diffraction, and was in good agreement with previously published results.^{2,4} There is a smooth transition from the cubic MgCu_2 -type to the hexagonal MgZn_2 -type structure at $x \approx 0.25$. We were able to obtain a cubic⁵ and probably a hexagonal allotrope of the $\text{Zr}(\text{Al}_{0.825}\text{Fe}_{0.175})_2$ compound monitored by the number of

arc-furnace remeltings. One of the samples ($x=0.2$) was measured before and after annealing at 1000°C for several days. The Mössbauer spectra were not sensitive to the allotropic transformation or to the annealing procedure. The Mössbauer studies of thin samples (less than 0.05 mg $^{57}\text{Fe}/\text{cm}^2$) at temperatures 90, 298, 303, 423, 433, and 612 K were performed using a constant acceleration spectrometer and a 50-mCi $^{57}\text{Co}/\text{Rh}$ radioactive source. Some of the experimental spectra at 90, 298, and 423 K are shown in Figs. 1–3. The spectra at 612 K all look like the high- x value spectra at 423 K.

III. ANALYSIS OF EXPERIMENTAL RESULTS AND DISCUSSION

Spectra in the paramagnetic state

The Mössbauer spectra in Figs. 2 and 3 in the paramagnetic state ($x \geq 0.2$) display a gradual change in the shape as a function of x . The spectra were analyzed as composed of seven subspectra corresponding to the number of Al first-nearest neighbors to the iron nucleus. It was assumed that the isomer shift and quadrupole interaction are linearly dependent on the number of Al neighbors. It was also assumed that Fe and Al in $\text{Zr}(\text{Al}_x\text{Fe}_{1-x})_2$ are randomly distributed, thus using a binomial expression for the probabilities of the number of Al neighbors (0–6 in identical positions relative to the central Fe nucleus).

The change in isomer shift per replacement of one Fe neighbor by Al is determined to be $+0.056(3)$ mm/sec,

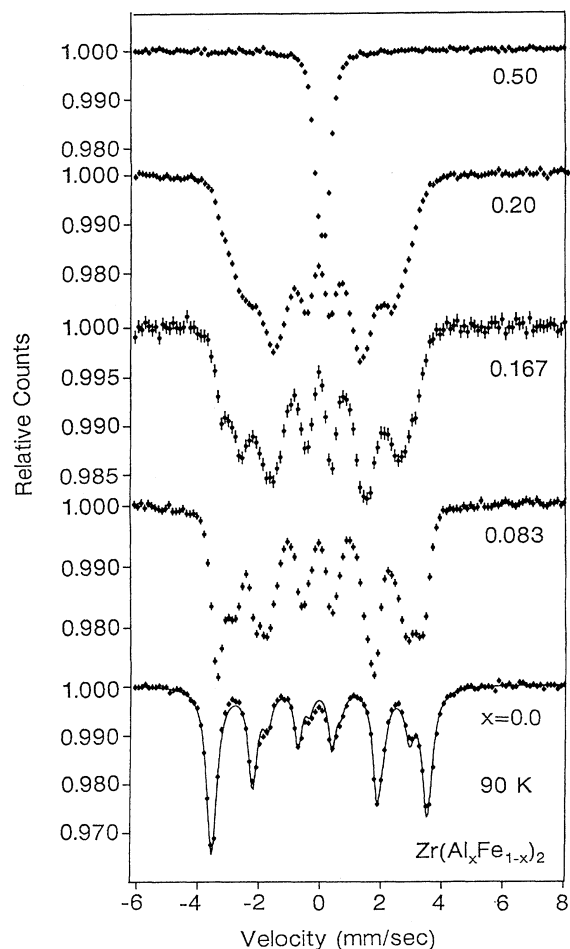


FIG. 1. Mössbauer spectra of ^{57}Fe in $\text{Zr}(\text{Al}_x\text{Fe}_{1-x})_2$ at 90 K.

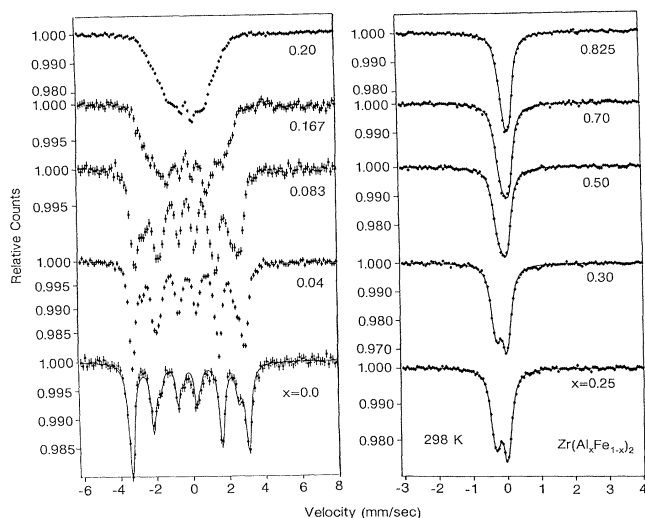


FIG. 2. Mössbauer spectra of ^{57}Fe in $\text{Zr}(\text{Al}_x\text{Fe}_{1-x})_2$ at 298 K.

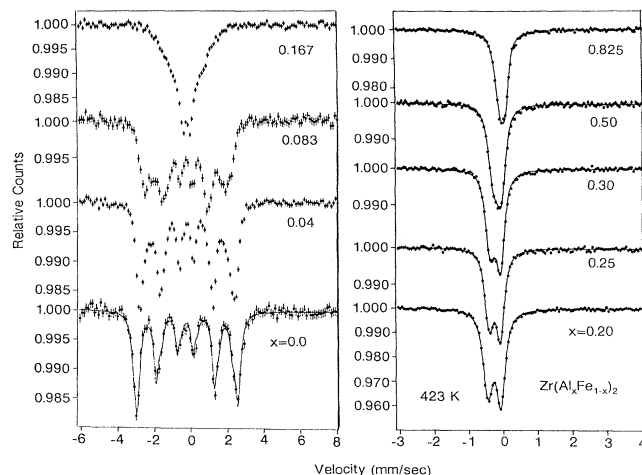


FIG. 3. Mössbauer spectra of ^{57}Fe in $\text{Zr}(\text{Al}_x\text{Fe}_{1-x})_2$ at 423 K.

and the respective change in quadrupole interaction is $-7.0(2)\%$, decreasing when Al replaces Fe.

The observed increase in isomer shift, when Al substitutes for Fe as first-nearest neighbors, indicates that the Al neighbor contributes to the electronic charge density in the central Fe nucleus less than an Fe neighbor. This observation and the observation that the electric field gradient acting on the Fe nucleus also decreases when Al substitutes for Fe as first-nearest neighbor can be understood in terms of the larger ionic radius of Al relative to Fe.

In Fig. 4 we see the change in isomer shift and quadrupole interaction of those iron nuclei with no Al neighbors, as a function of x . We observe that the isomer shift is independent of x , and does not change when the crystal structure changes from cubic to hexagonal. Its temperature dependence is fully consistent with the expected thermal shift.⁶ On the other hand, the quadrupole interaction experienced by the iron nucleus with no Al neighbors displays a decrease at the crystallographic phase transition and is almost temperature independent.

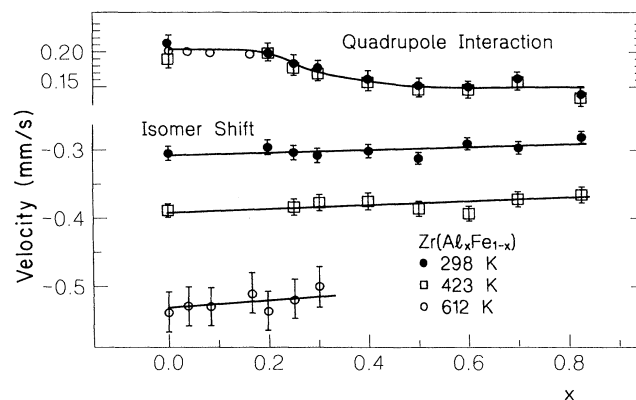


FIG. 4. The isomer shift and quadrupole interaction of ^{57}Fe with no Al as first-nearest neighbor in $\text{Zr}(\text{Al}_x\text{Fe}_{1-x})_2$ at 298, 423, and 612 K.

Spectra in a magnetically ordered state

It is obvious from Figs. 1–3 that $\text{Zr}(\text{Al}_x\text{Fe}_{1-x})_2$ for $x \leq 0.20$ orders magnetically at relatively high temperatures, above room temperature.² Below T_c the Mössbauer spectra of ZrFe_2 exhibit two well-defined six-line pattern subspectra with an intensity ratio of 3:1, as expected for an easy axis of magnetization along the [111] axis.⁷ The spectra were fitted under this assumption, and thus the free hyperfine parameters, were only the quadrupole interaction ($\frac{1}{4}eqQ = 0.2$ mm/s) and the two magnetic hyperfine fields, 219 and 203 kOe at 90 K, 202 and 188 kOe at 298 K, and 171 and 168 kOe at 423 K. This decrease in hyperfine fields as a function of temperature approximately follows a spin- $\frac{5}{2}$ Brillouin function, assuming $T_c = 630$ K.² The spectra for $\text{Zr}(\text{Al}_x\text{Fe}_{1-x})_2$, $0 < x < 0.25$, Figs. 1–3 exhibit a large distribution of hyperfine fields on top of the distribution of isomer shift and quadrupole interaction discussed above. This distribution may also result from Al first-nearest neighbors. In addition, the local presence of Al neighbors affects the iron local magnetic anisotropy, leading to a distribution of local iron magnetic-moment orientations.

Softening phenomena

Finally we come to the problem of possible phonon softening. In order to test the change in Debye temperature (Θ_D) as a function of x , we measured very accurately three ratios of the Mössbauer spectral areas at two temperatures, 298 and 423 K, 303 and 433 K, and 303 and 612 K. Since we used relatively thin absorbers (less than 0.05 mg $^{57}\text{Fe}/\text{cm}^2$), the spectral area is almost proportional to the Mössbauer recoil-free fraction $f(T)$ of the absorber. The nonlinearity can be corrected by well-known methods. The spectral area is proportional to the expression⁸

$$A(z) = ze^{-z} [I_0(z) + I_1(z)], \quad (1)$$

where $z = \frac{1}{2}t_a$, $t_a = n(^{57}\text{Fe})\sigma_0 f(T)$. t_a is the dimensionless thickness of the absorber, $n(^{57}\text{Fe})$ is the number of ^{57}Fe nuclei in the unit area of the absorber, σ_0 is the nuclear resonance cross section, and I_n are modified Bessel functions. An approximate estimate of t_a allows the calculation of $A(\frac{1}{2}t_a)$ and its deviation from $\frac{1}{2}t_a$ itself, Fig. 5. In most of our cases these nonlinearity corrections for a doublet spectrum were less than 12%, much less for a magnetically split spectrum. The correction for the ratio of spectral areas was certainly less than for the areas themselves; it was less than 5% in the most extreme case.

In the Debye model approximation $f(T)$ depends, besides on the nuclear properties, only on the Debye temperature of the crystal:

$$f(T) = \exp \left\{ -\frac{6E_R}{k\Theta_D} \left[\frac{1}{4} + \left(\frac{T}{\Theta_D} \right)^2 \int_0^{\Theta_D/T} \frac{z}{e^z - 1} dz \right] \right\}, \quad (2)$$

where E_R is the nuclear recoil energy.

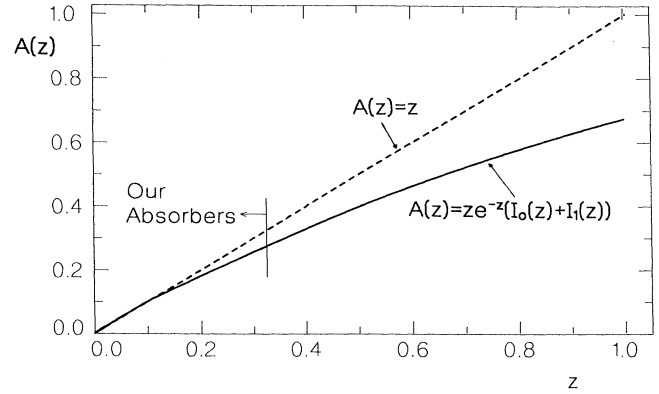


FIG. 5. The relation between the spectral area of a single Mössbauer Lorentzian absorption line and the dimensionless thickness of the absorber t_a .

Since the Mössbauer spectral area, even when corrected for absorber thickness, is only proportional to f , a single-temperature Mössbauer measurement is not enough to determine Θ_D . However, two measurements at two different temperatures enable the reduction of Θ_D from the ratio of the spectral areas. A major advantage of this procedure is that one avoids most of the uncertainties in absorber thickness and in calculating the non-resonant background corrections, all necessary for determining absolute values of the recoil-free fractions. To test the validity of this procedure we measured iron metal (25 μm thick) at the three sets of two temperatures. After

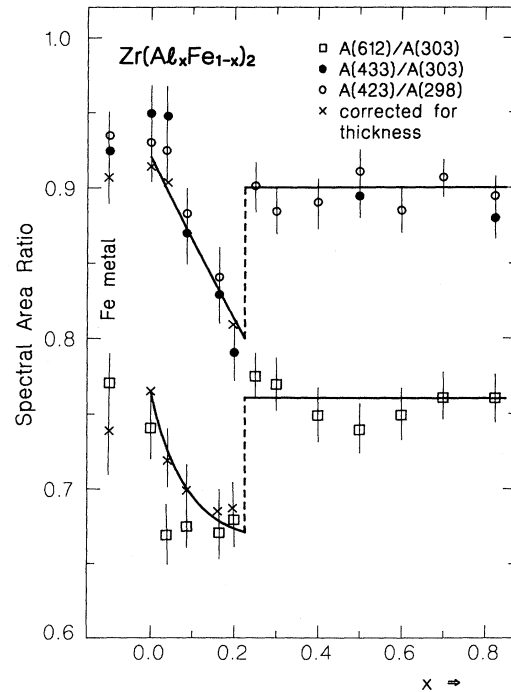


FIG. 6. The ratios of spectral areas for pairs of temperatures of ^{57}Fe in $\text{Zr}(\text{Al}_x\text{Fe}_{1-x})_2$.

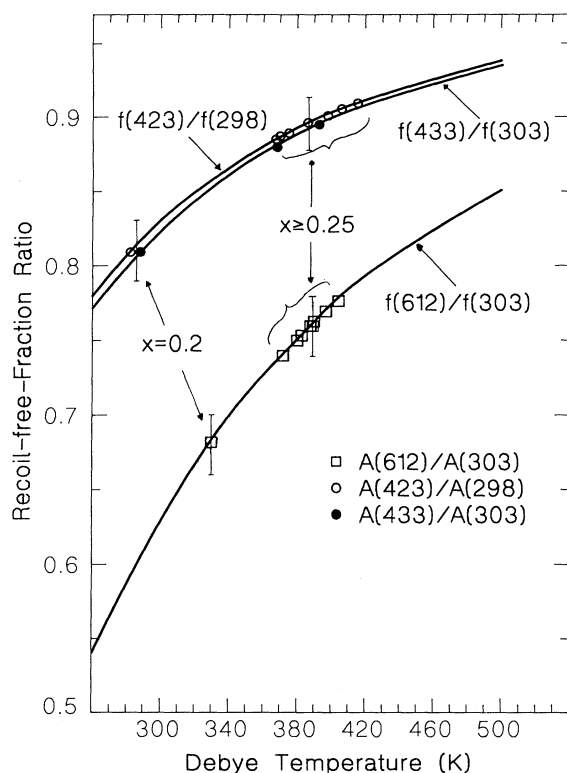


FIG. 7. The correspondence between the ratio of the ^{57}Fe recoil-free fractions at 423 and 298 K, 433 and 303 K, and 612 and 303 K and the Debye temperatures of $\text{Zr}(\text{Al}_x\text{Fe}_{1-x})_2$.

correcting for thickness the ratios for the three pairs of temperatures correspond to $\Theta_D \approx 390 \pm 20$ K in perfect agreement with the value obtained from a full temperature dependence of the recoil free fraction and isomer shift.⁹ The ratios of the experimental spectral areas of $\text{Zr}(\text{Al}_x\text{Fe}_{1-x})_2$ were corrected for finite thickness in

those cases where it was absolutely necessary. Mostly these were the cases where at one temperature the spectrum is magnetically split and at the other temperature it is a pure quadrupole doublet. The experimentally measured ratio of the spectral areas of $\text{Zr}(\text{Al}_x\text{Fe}_{1-x})_2$, Fig. 6, assisted by the theoretical curves given in Fig. 7, yield the corresponding Debye temperatures. One obtains that for the Al-rich hexagonal compounds, all three ratios yield almost the same Debye temperature, $\Theta_D = 395 \pm 20$ K. This proves that for these compounds the Debye model is valid up to 612 K. For the Al poor ($x \leq 0.2$) cubic compounds as well as for pure ZrFe_2 and Fe metal itself, the ratios $f(433\text{K})/f(303\text{K})$ and $f(612\text{K})/f(303\text{K})$ yield slightly different Debye temperatures. However, the dependence of the two ratios on Al concentration exhibit the same behavior, softening of the crystal up to $x = 0.2$, the effective Debye temperature decreases from $\Theta_D = 440$ K for $x = 0$ to $\Theta_D \approx 310$ K for $x = 0.2$. At the crystallographic phase transition (between $x = 0.2$ and 0.25) there is an abrupt increase in Θ_D to the constant value of the Al-rich hexagonal structure, 395 K. However, since the Al-rich absorbers contained less ^{57}Fe , thickness corrections (not done for these absorbers) will lead to a slight increase of Θ_D as a function of x . This general behavior confirms the expectations³ suggested by the data of the Ni bonding strength of Ni in $\text{LaNi}_{5-x}\text{Al}_x$ and the hydrogen sorption properties of $\text{Zr}(\text{Al}_x\text{Fe}_{1-x})_2$ (Ref. 4) and $\text{LaNi}_{5-x}\text{Al}_x$ (Ref. 10).

ACKNOWLEDGMENT

This work was partly supported by the Basic Research Foundation administered by the Israel Academy of Sciences and Humanities.

¹H. R. Kirchmayr and C. A. Poldy, *Handbook on the Physics and Chemistry of Rare Earths*, edited by K. A. Gschneider, Jr. and L. Eyring (North-Holland, Amsterdam, 1979), Chap. 14.

²Y. Muraoka, M. Shiga, and Y. Nakamura, *Phys. Status Solidi A* **42**, 369 (1977).

³I. Jacob, R. Moreh, O. Shahal, A. Wolf, and Z. Gavra, *Phys. Rev. B* **38**, 7806 (1988).

⁴I. Jacob and D. Shaltiel, *Solid State Commun.* **27**, 175 (1978).

⁵Powder diffraction file, compiled and published by the joint committee on powder diffraction standards (JCPDS), International Center for Diffraction Data (ICDD), 1601 Park Lane, Swarthmore, PA 19081, 1988, entry 30/26; Markiv and Kri-

pyakevich, *Kristallogr.* **11**, 859 (1966).

⁶B. D. Josephson, *Phys. Rev. Lett.* **4**, 341 (1960).

⁷U. Atzmony, M. D. Dariel, E. R. Bauminger, D. Lebenbaum, I. Nowik, and S. Ofer, *Phys. Rev. Lett.* **28**, 244 (1972).

⁸N. Abe and L. H. Schwartz, in *Mössbauer Effect Methodology*, edited by I. J. Gruverman and C. W. Seidel (Plenum, New York, 1973), Vol. 8, p. 249. Also J. M. Williams and J. S. Brooks, *Nucl. Instrum. Methods* **128**, 363 (1975).

⁹R. S. Preston, S. S. Hanna, and J. Heberle, *Phys. Rev.* **128**, 2207 (1962).

¹⁰M. H. Mendelsohn, D. M. Gruen, and A. E. Dwight, *Nature (London)* **269**, 45 (1977); see also *J. Less-Common Metals* **63**, 193 (1979).